

TAT
C6
CER 69-70-13
COPY 2

G. E. - R. R. COPY

WIND STUDY OF KAISER CENTER
OFFICE BUILDING

by
G. Hsi¹, J. E. Cermak² and W. Z. Sadeh³

for

Metronics Associates, Inc.
3201 Porter Drive
Stanford Industrial Park
Palo Alto, California



**FLUID MECHANICS PROGRAM
ENGINEERING RESEARCH CENTER
COLLEGE OF ENGINEERING
COLORADO STATE UNIVERSITY
FORT COLLINS, COLORADO**

WIND STUDY OF KAISER CENTER
OFFICE BUILDING

by
G. Hsi¹, J. E. Cermak² and W. Z. Sadeh³

for

Metronics Associates, Inc.
3201 Porter Drive
Stanford Industrial Park
Palo Alto, California

Fluid Mechanics Program
Fluid Dynamics and Diffusion Laboratory
College of Engineering
Colorado State University
Fort Collins, Colorado

September 1969

CER69-70GH-JEC-WZS-13

-
- 1 Research Associate
2 Professor-in-Charge, Fluid Mechanics Program
3 Assistant Professor of Engineering



U18401 0575413

ABSTRACT

Mean and fluctuating wind loading on a 1:192 scale model of Kaiser Center Office Building 403 ft high was studied in an uniform flow. Pressure measurements were carried out for four different wind directions (N, NE, E, and S). The wind loading was influenced strongly by a tall building immediately to the southeast when the wind was from the south.

Generally, the mean pressure was higher at the center portion of an upwind face than near its edges. On the leewind surface relatively uniform negative pressure (suction) was obtained. Its absolute value was about one-third of that along an upwind face. On the other hand, the fluctuating pressure was highest near the building base, in the flow separation region and in the wake of the adjacent building in a southerly wind.

A model of the upstream topography to the northeast was constructed using a 1:600 scale. This model terrain was 24 ft long (2.7 miles of the prototype terrain) with the Kaiser building site near its trailing edge. Mean velocity and turbulence intensity profiles were measured along the terrain.

ACKNOWLEDGMENTS

This study was supported by Metronics Associates, Inc. Mr. J. A. Garrison assisted in constructing the model buildings and experimental apparatus.

TABLE OF CONTENTS

	<u>Page</u>
ABSTRACT	ii
ACKNOWLEDGMENTS.	iii
LIST OF FIGURES.	v
LIST OF SYMBOLS.	vi
1. INTRODUCTION	1
2. EXPERIMENTAL APPARATUS	2
2.1 The Model Building.	2
2.2 Upstream Topography Model	3
3. EXPERIMENTAL TECHNIQUE AND INSTRUMENTATION	4
3.1 Pressure and Velocity Measurement	4
3.2 Turbulence Intensity Measurement.	5
4. RESULTS.	6
4.1 Mean Velocity Survey.	6
4.2 Turbulence Intensity Survey	8
4.3 Pressure Survey	8
4.3.1 Pressure survey for N wind	10
4.3.2 Pressure survey for NE wind.	10
4.3.3 Pressure survey for E wind	11
4.3.4 Pressure survey for S wind	11
5. CONCLUSIONS	13
REFERENCES	14

LIST OF FIGURES

<u>Figure</u>		<u>Page</u>
2.1	Sketch of the model-buildings arrangement and the low-speed wind tunnel	15
2.2	Sketch of the topography model.	16
2.3	Pressure taps location and sketch of wind directions used	17
2.4	View of the Kaiser building model	18
2.5	Sketch of the field topography.	19
3.1	Simplified block diagram of the pressure-transducer measurement system	20
3.2	General view of the pressure measurement system	21
4.1	Velocity variation with height at station 1	22
4.2	Velocity variation with height at station 2	23
4.3	Velocity variation with height at station 3	24
4.4	Velocity variation with height at station 4	25
4.5	Turbulence intensity profiles along NE topography model based on local mean velocity	25
4.6	View of building model; N, NE and E wind.	27
4.7	View of building model; S wind	28
4.8	Mean pressure coefficient; N wind	29
4.9	Peak pressure coefficient; N wind	30
4.10	Mean pressure coefficient; NE wind.	31
4.11	Peak pressure coefficient; NE wind.	32
4.12	Mean pressure coefficient; E wind	33
4.13	Peak pressure coefficient; E wind	34
4.14	Mean pressure coefficient; S wind	35
4.15	Peak pressure coefficient; S wind	36
4.16	Fluctuating pressure coefficient; S wind.	37

LIST OF SYMBOLS

Symbol

c_p	Mean pressure coefficient
c_{p_f}	Fluctuating pressure coefficient
$c_{p_{max}}$	Instantaneous peak pressure coefficient
d	Nominal diameter of the hot wire
l	Hot-wire length
p	Total local pressure
Tu_x	Longitudinal turbulence intensity
U	Wind velocity
u	Fluctuating velocity parallel to the mean flow velocity
x, y, z	Coordinates
α	Exponent in Eq. (1)
δ	Boundary-layer thickness
ρ	Air density

Superscripts

'	Means fluctuating values
---	--------------------------

Subscript

G	Gradient velocity height
max	Half of instantaneous peak-to-peak fluctuating value
rms	Root-mean-square
∞	Free-stream

1. INTRODUCTION

The mean and fluctuating wind loadings on a tall building can be accurately studied in an appropriate wind tunnel. With well established knowledge on modeling criteria and controlled flow characteristics in a wind tunnel, model tests provide useful information for designing tall buildings.

The main purpose of this study was to find the aerodynamic forces on the proposed Kaiser Center Office Building (K.B.) by means of measurements on a model. A significant, arc-shaped, tall surrounding building (S.B.) is situated SE of the K.B. It affected strongly the aerodynamic forces for certain wind directions. Models of both buildings (K.B. and S.B.), using the same modeling scale, were installed on a rotating disc. The latter was placed on the wind tunnel floor.

Detailed measurements of the pressure distribution on the K.B. model for four wind directions N, NE, E and S were made. The critical wind direction, i.e., the wind direction for which the largest peak pressure occurred, was found. An uniform air flow (no boundary layer) was used in performing the pressure measurements on the isolated building models. The motivation of this approach was to provide pressure distribution which could easily be corrected for any assumed approaching wind velocity profile.

A model of the NE topography with respect to the Kaiser building site was also constructed. The mean velocity and turbulence intensity in a relatively thick and turbulent boundary layer along it was investigated.

2. EXPERIMENTAL APPARATUS

The aim of this study was to obtain the local wind loading, i.e., the pressure distribution, on a model of the Kaiser Center Office Building in Oakland. The variation of velocity and turbulence intensity profiles along the upstream NE topography with respect to the K.B. site was also studied. Sketches of the experimental arrangement of the model building and topography are shown in Figs. 2.1 and 2.2, respectively.

The K.B. model was tested in uniform flow employing a low-speed wind tunnel. On the other hand, the topography model was studied in a thick, turbulent boundary layer using a suitable micrometeorological wind tunnel. Both wind tunnels are located in the Fluid Dynamics and Diffusion Laboratory, Colorado State University [1,2].

2.1 The Model Building

The K.B. model was made of "Lucite" 0.375 in. thick using a scale of 1:192. A sketch of the model is portrayed in Fig. 2.3 which also shows all important dimensions and the flow directions used. Pressure taps 1/16-in. diameter were drilled on building faces along ten particular floors. They were located as follows: 40 on half of wall 1-2, 25 on wall 2-3, 20 on wall 3-4, 10 on wall 4-5, 20 on wall 5-6, 25 on wall 6-7 and 40 on half of wall 7-8. Note that the face 7-8 and 1-2 are identical. A total of 180 pressure taps were drilled along half of the building. Pressure-tap locations can be found by using the scale shown in Fig. 2.3. In order to measure the pressure distribution along the other half of the building, it was necessary to rotate it by 180°. Hence, it was possible to monitor the pressure on

the model at 360 stations. No pressure taps were bored on the building roof. Photographs of the K.B. model are displayed in Fig. 2.4.

The tall, arc-shaped building located SE of the K.B. was constructed of styrofoam to a scale of 1:192. It is also shown in Fig. 2.3. Both model buildings were mounted on a rotatable plywood disc. For investigating the critical wind direction (wind direction producing strongest pressure fluctuation on K.B.), the disc was rotated through 360°.

2.2 Upstream Topography Model

A model simulating the NE upstream topography with respect to the K.B. site was constructed. This is the only direction for which a significant topographic variation exists. This topographic relief rises about 175 ft over a distance of 2500 ft. A sketch showing the location of K.B. relative to the local topography is portrayed in Fig. 2.5.

This model was built using a scale of 1:600. Its total length was 24 ft corresponding to 2.7 miles of the upstream field topography. It is displayed in Fig. 2.2 which also shows the system of coordinates used, all important dimensions and the location of the measurement stations. The first 12 ft of the model was made of cardboard whereas the last 12 ft (near the K.B. site) of styrofoam. Its leading edge was smoothly joined to the wind-tunnel floor by means of a smooth transition slope (see Fig. 2.2).

3. EXPERIMENTAL TECHNIQUE AND INSTRUMENTATION

3.1 Pressure and Velocity Measurement

The mean pressure on the model faces was measured by means of an electronic pressure meter (Trans-Sonic, Type 120A). The fluctuating and instantaneous peak pressure were obtained by using low-pressure differential pressure transducers (Statham, model PM283). Six identical pressure transducers were installed inside the model and connected closely to the pressure taps (1).

The pressure mean and its fluctuating components, were measured with respect to the static pressure of the free-stream. A Pitot-static tube located 2.07 ft above the model, as shown in Fig. 2.1, was employed to measure the latter. It was also employed for measuring the uniform flow speed.

In connection with these measurements the following auxiliary equipment was used: a variable range Dana amplifier (Model 3500), a seven-channel Mincom tape recorder (Type 100), a Bruel and Kjaer true RMS meter (Type 2416), a General Radio wave analyzer (Type 1911-A), a dual-beam Tektronix storage oscilloscope (Type 564), a x-y plotter (F.L. Mosely Co., Model 135) and a digital voltmeter (Hewlett-Packard, Model 3440A). A simplified block diagram of the pressure-transducer system is shown in Fig. 3.1 and a general view of the auxiliary equipment is provided by Fig. 3.2.

The velocity along the topography model was measured using a Pitot-static tube and the same Trans-Sonic pressure meter. This was accomplished by moving the probe continuously by means of an electrically operated traversing mechanism. The vertical variation of velocity was recorded by a x-y plotter (F.L. Mosely Co., Model 135).

3.2 Turbulence Intensity Measurement

The longitudinal turbulence intensity along the topography model was measured by means of a single hot-wire anemometer. When performing these measurements, the hot-wire probe was positioned by means of the traversing mechanism. The measurements were performed using a Disa hot-wire anemometer (Type 55A01). A tungsten wire of 0.00025 in. nominal diameter and aspect ratio, ℓ/d , of 240 (ℓ being the wire length and d its diameter) was employed. In connection with the hot-wire unit a Bruel and Kjaer true RMS meter (Type 2416), a dual-beam Tektronix storage oscilloscope (Type 564) and a Hewlett-Packard digital DC voltmeter (Model 3440A) were used.

Generally, the experimental technique and instrumentation used during this investigation are similar to those described in Ref. 1.

4. RESULTS

The following information was obtained during the course of this experimental investigation:

- (1) The critical wind direction, i.e., the direction for which the instantaneous peak pressure acting on the K.B. model is the largest.
- (2) Mean and instantaneous peak pressure on the K.B. model in N, NE and E wind directions.
- (3) Mean, fluctuating and instantaneous peak pressure in the critical wind direction.
- (4) Velocity and longitudinal turbulence intensity along the topography model.

4.1 Mean Velocity Survey

The upstream wind velocity gradient is a major factor in determining the wind loading on the building. The K.B. model was studied in an uniform flow and, therefore, velocity profiles obtained along the upstream topography provide the pertinent information necessary for computing the mean pressure coefficient on the upwind faces of the K.B. model. The mean pressure acting on the building is proportioned to the square of the local velocity. Then, the boundary-layer flow pressure coefficient, $c_{p_{bl}}$, is related to the uniform flow pressure coefficient, c_{p_u} , by the following relationship:

$$c_{p_{bl}} = c_{p_u} \left(\frac{z}{\delta} \right)^{2\alpha} \quad (1)$$

In this equation z is the height, δ the boundary-layer thickness and α the exponent obtained from the power-law variation of velocity profile. The latter is given by

$$\frac{U}{U_{\infty}} = \left(\frac{z}{\delta}\right)^{\alpha}, \quad (2)$$

where U stands for the velocity and U_{∞} is the free stream (uniform) velocity.

The value of α depends on the upstream topographic conditions [3]. The measurements along the topography model were conducted under zero pressure gradient conditions. The latter was obtained by adjusting the ceiling of the micrometeorological wind tunnel [2]. Free-stream velocities of 30, 49 and 68 fps were used. The mean velocity and turbulence intensity were measured at stations 1, 3 and 4 (see Fig. 2.2). Station 2 was used to determine if flow separation existed immediately downstream from the leading edge. It was found that the velocity profile was smooth and no inflection point was monitored. Therefore, separation was not present.

The velocity change with height at the four measurement stations are displayed in Figs. 4.1 to 4.4. The values for α and δ (see Eq. (2)) at the four measuring stations are summarized below:

Station	α	δ (in.)
1	0.180	18.5
2	0.112	14.2
3	0.174	20.0
4	0.152	24.0

The field velocity profile may be represented by [3]

$$\frac{U}{U_G} = \left(\frac{z}{z_G}\right)^{\alpha}, \quad (3)$$

where U_G is the velocity at gradient velocity height z_G . Note that U_g and z_g are equivalent to U_{∞} and δ in the wind tunnel study.

The results found in the wind-tunnel study agree with findings for flat open terrain presented in Ref. 3. In the latter for flat open country $\alpha = 0.16$ and $z_G = 900$ ft.

4.2 Turbulence-Intensity Survey

The turbulence intensity based on local mean velocity

$$Tu_x = \frac{u_{rms}(z)}{U(z)}, \quad (4)$$

was measured. The fluctuating velocity u is parallel to the mean flow velocity U , and the subscript rms denotes the square-root of the mean-square (time-averaged) value, i.e., $(\overline{u^2})^{1/2}$.

The results along the topography model at stations 1, 3 and 4 and at $U_\infty = 50$ fps are shown in Fig. 4.5. They were reproducible within 2 to 3%. A maximum turbulence intensity of 0.10 was measured at $z/\delta = 0.09$ at station 1. At $z/\delta = 0.22$ roughly same turbulence intensity of 7% was measured at all three stations. The free stream turbulence intensity was about 0.7%.

4.3 Pressure Survey

A detailed survey of the pressure along the K.B. model building (1:192 scale) in an uniform flow was carried out for four wind directions (N, NE, E and S) at a constant upstream velocity U_∞ of 50 fps. General views of the building model for N, NE and E wind are shown in Fig. 4.6 whereas for S wind in Fig. 4.7. The static pressure of the free stream was used as reference for measuring mean, fluctuating and instantaneous peak pressure. It was monitored by means of a Pitot-static tube (see Fig. 2.1).

The following definitions are used for presenting pressure results [1]:

- (1) local mean pressure coefficient

$$c_p = \frac{\overline{\Delta p}}{\frac{1}{2}\rho U_\infty^2}, \quad (5)$$

- (2) fluctuating pressure coefficient

$$c_{P_f} = \frac{P_{rms}}{\frac{1}{2}\rho U_\infty^2}, \quad (6)$$

- (3) peak pressure coefficient

$$c_{P_{max}} = \frac{P'_{max}}{\frac{1}{2}\rho U_\infty^2}. \quad (7)$$

In the above relationships $\overline{\Delta p}$ is the mean (time averaged) of the difference between the local mean pressure and the free-stream static pressure, P_{rms} denotes square-root of mean square fluctuating pressure, P'_{max} is half of instantaneous peak-to-peak fluctuating pressure and ρ is the air density ($\rho = 0.00187$ slug/ft³ at the laboratory elevation).

The critical wind direction was found rotating the model by 45° steps through one revolution. Then, it was defined to be the angle at which the largest peak pressure on K.B. model was observed.

Main features of the pressure distribution for each flow direction are summarized in the following sections.

4.3.1 Pressure survey for N wind

In this case the wind is normal to the north wall, i.e., face 2-7. The mean and peak pressure coefficient distribution along the model building faces are displayed in Figs. 4.8 and 4.9, respectively. High mean pressure was found at the center portion of the upwind faces (north wall). Along its concave part (faces 3-4, 4-5, and 5-6), same values of mean pressure as on faces 2-3 and 6-7 were measured. However, a 50% decrease near the edges 2-2 and 7-7 was observed. Flow separation occurred along these two edges. Near the latter high negative pressure was measured. The pressure became smaller along the side faces 2-1 and 7-8 (west and east walls) farther downstream. On the leeward face (south wall), negative pressure coefficients of approximately same value were observed at all stations. Their absolute value was about one-third of the mean pressure coefficient on the upwind face.

The peak pressure coefficients were found to be largest near the building base and edges. High values were observed at the edges 1-1 and 8-8. Along the upwind faces, it was less than or equal to one-fifth of the local mean pressure coefficient. On the other hand, on the leeward surfaces the peak pressure and the mean pressure coefficient were about the same order of magnitude.

The surrounding building had negligible influence on the pressure measurements for this wind direction. This was also true for the NE and E wind directions.

4.3.2 Pressure survey for NE wind

In this case the flow approached the edge 7-7 and deflected along faces 7-6 and 7-8. The mean pressure distribution is portrayed in Fig. 4.10. The highest mean pressure coefficient (0.90) was observed near

edge 7-7. It decreased towards the trailing edges of the upwind faces (north and east walls). Along the leewind faces (south and west walls), it varied between -0.40 to -0.60.

At most of the stations the peak pressure coefficients were less than 0.25 as shown in Fig. 4.11. They were relatively higher near the building base. The largest peak pressure coefficient, 0.50, was found near the edge 1-1 on the face 1-2 (west wall).

4.3.3 Pressure survey for E wind

The flow was perpendicular to the face 7-8 (east wall). On the upwind face (face 7-8) the mean pressure coefficients were higher at the center portion and showed a 42% decrease at edges 7-7 and 8-8 as displayed in Fig. 4.12. Flow separation occurred at these two edges. Along the side and leewind faces, negative mean pressure prevailed. Their values varied from -0.22 to -0.33. Evidently, the surrounding building did not exert any influence on the pressure measurements. The results on the upwind and leewind faces were similar to those in N wind.

Peak pressure coefficients are portrayed in Fig. 4.13. They are smaller on the upwind face and become larger near the base and on the leewind face. The largest peak pressure was about 0.54 near the base on face 7-8 in this wind direction.

4.3.4 Pressure survey for S wind

The largest peak pressure on a building may be caused by the local turbulence generated by the surrounding building, by the turbulence generated in flow over the upstream terrain or by local flow instabilities produced by the building geometry. This study revealed that the upstream building (S.B.) produced a wake for a S wind which caused maximum pressure fluctuation on the K.B. The model buildings were

rotated by 45° increments, with respect to the approaching wind, through one revolution. It was found that the largest peak pressure occurred for the S wind direction, in which the wake of the upstream building extended over about half of the model building (K.B.). The flow pattern was complex and the fluctuating and instantaneous peak pressures were in general very high.

The results for the mean, fluctuating and instantaneous peak pressure are displayed in Fig. 4.14, 4.15 and 4.16, respectively. On the upwind faces, the wake of the upstream building covered approximately the lower half of the upwind faces (south wall), i.e., below the line from the upper corner 8 to the lower corner 1, (see Fig. 4.14). The side face 7-8 (east wall) was in the wake region whereas the other side, face 1-2 (west wall), was not. The mean pressure coefficients were negative and small in the wake region and along the leewind faces (north wall).

In contrast to the mean pressure coefficient, the peak pressure coefficient was larger in the wake region (see Fig. 4.15). The largest peak pressure coefficient was found to be 1.24 on face 12-1. The eddies shed by the upwind building were apparently impinging upon the lower part of face 12-1.

The fluctuating pressure coefficients are exhibited in Fig. 4.16. In general, they were equal to or less than 0.30. Only at the location where the largest peak pressure occurred, was the local fluctuating pressure coefficient larger -- a maximum of $c_{P_f} = 0.49$ was measured.

5. CONCLUSIONS

Mean pressure coefficients determined from measurements on a 1:192 scale model placed in an uniform flow provided reference values. These coefficients obtained for a N, NE, E and S wind can be used to obtain corresponding mean pressure coefficients for any height variation of mean velocity desired to be studied.

Wind speed profiles over a 1:600 scale model of gradually rising terrain NE of the Kaiser Building revealed that the terrain had negligible effect on the wind structure. For a NE wind the velocity profile at the building site was found to be essentially the same as for open flat terrain.

The fluctuating and instantaneous peak pressure loading on the Kaiser Building model in N, NE and E wind were primarily due to local geometrical features of the building. At the sharp corners separation of the flow occurred and produced local instabilities. For the S wind pressure fluctuations were primarily due to the wake of the upwind building. The latter effect resulted in higher levels of pressure fluctuations than the former. Thus, the influence of the upwind building should be accounted for in the design of the Kaiser Building windows and outer skin panels.

REFERENCES

1. Sadeh, W. Z., J. E. Cermak and G. Hsi, "A study of wind loading on tall structures--Atlantic-Richfield Plaza Buildings," CER68-69WZS-JEC-GH-36, Colorado State University (1969).
2. Cermak, J. E. and E. J. Plate, "Micrometeorological wind tunnel facility, description and characteristics," CER63EJP-JEC-9, Colorado State University (1963).
3. Davenport, A. G., "The dependence of wind loads on meteorological parameters," Proceedings, Vol. 1, Wind Effects on Buildings and Structures, University of Toronto Press, Ottawa, Canada (1967).

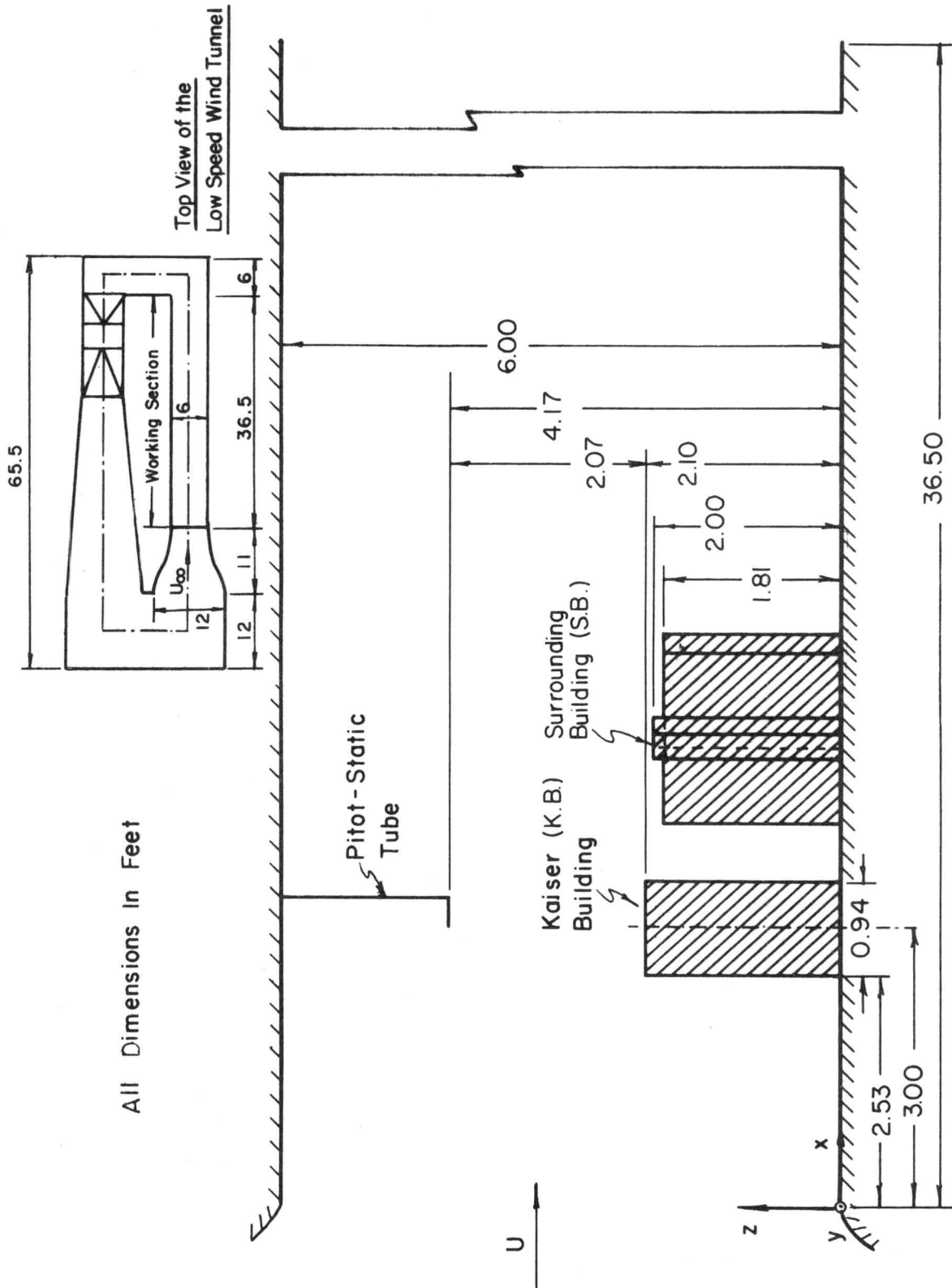


Figure 2.1 Sketch of the model-buildings arrangement and the low-speed wind tunnel.

Station	x	y	z
1	-5.00	0	0
2	2.66	0	0.70
3	17.66	0.46	0.25
4	23.74	0.46	0.14
K.B.	25.08	0.46	0.10

All Dimensions in Feet

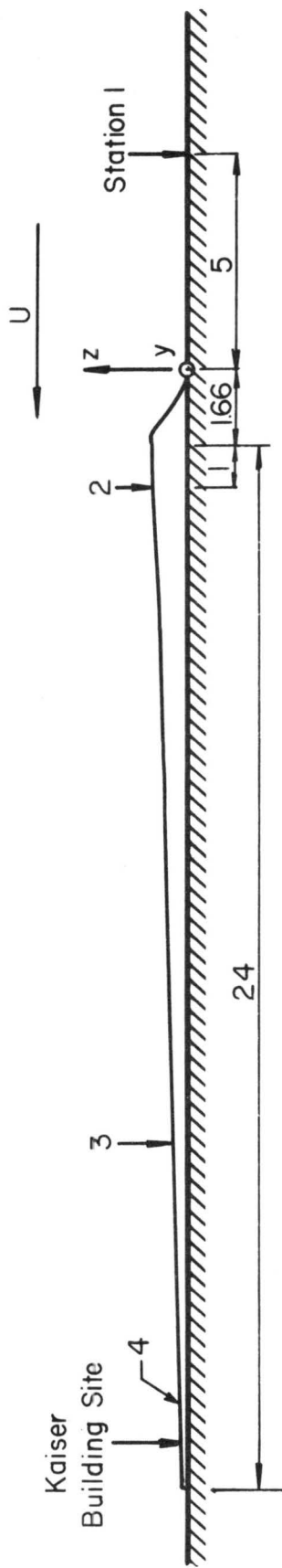


Figure 2.2 Sketch of the topography model.

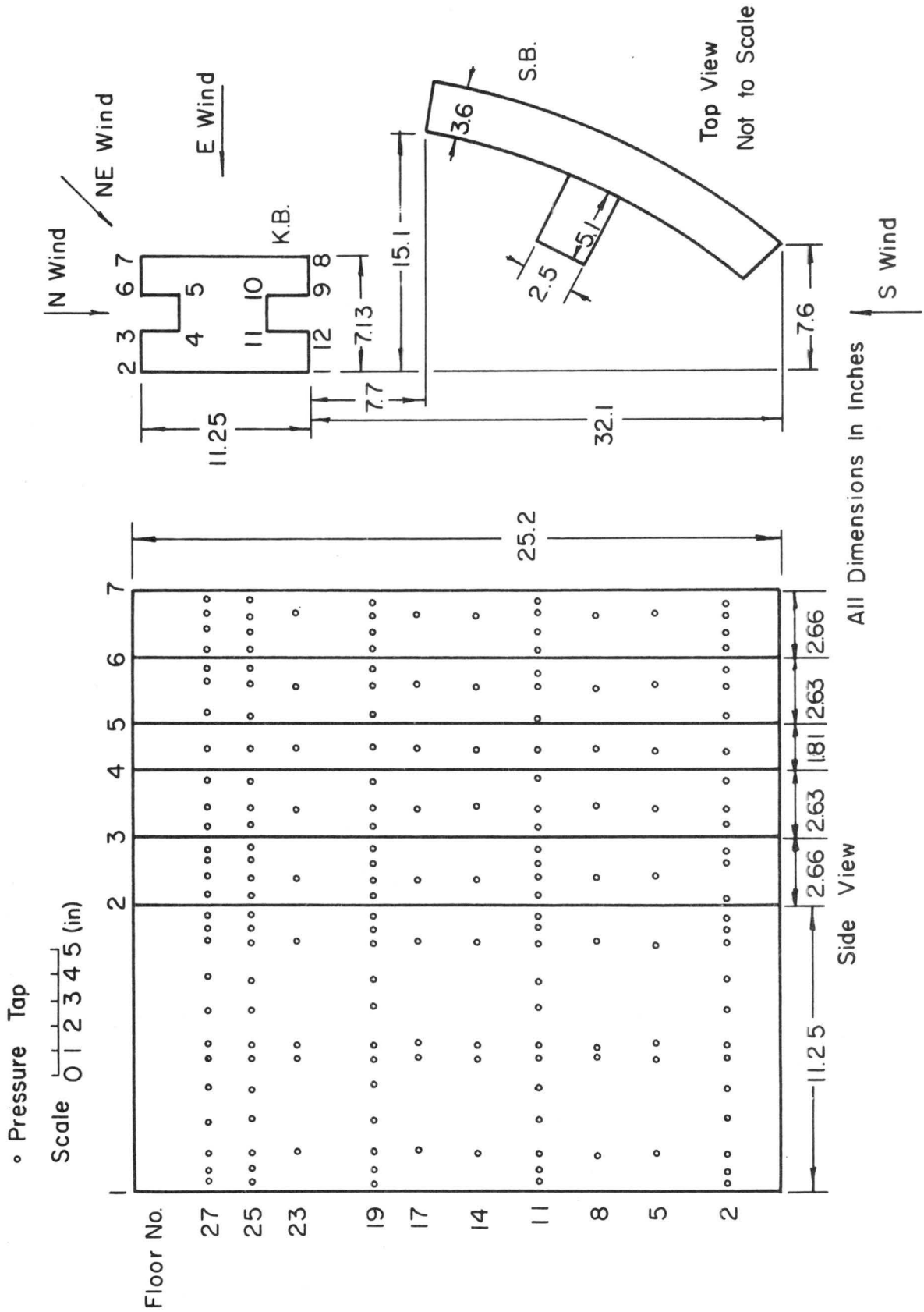
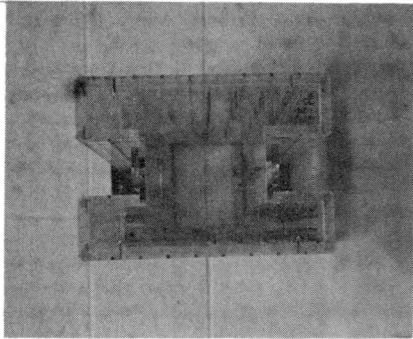
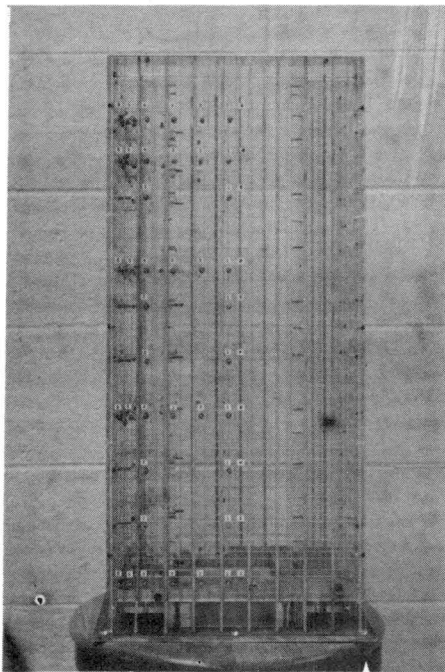


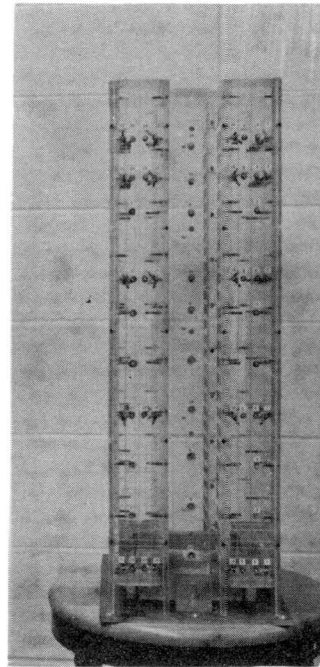
Figure 2.3 Pressure taps location and sketch of wind directions used.



Top View



Front View



Side View

Figure 2.4 View of the Kaiser building model.

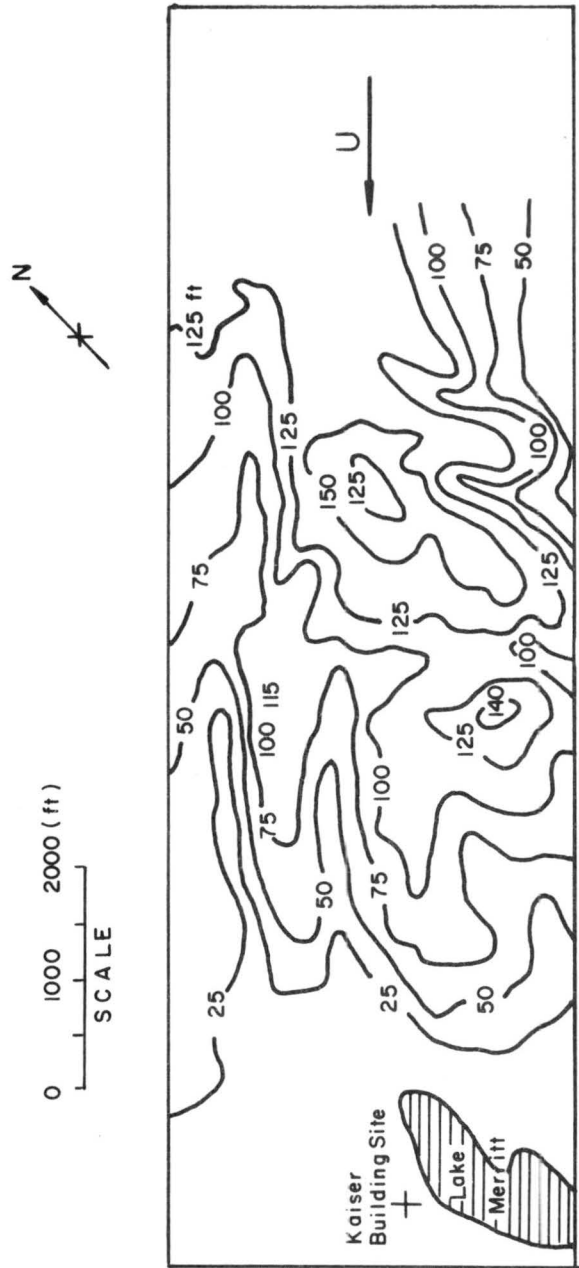


Figure 2.5 Sketch of the field topography.

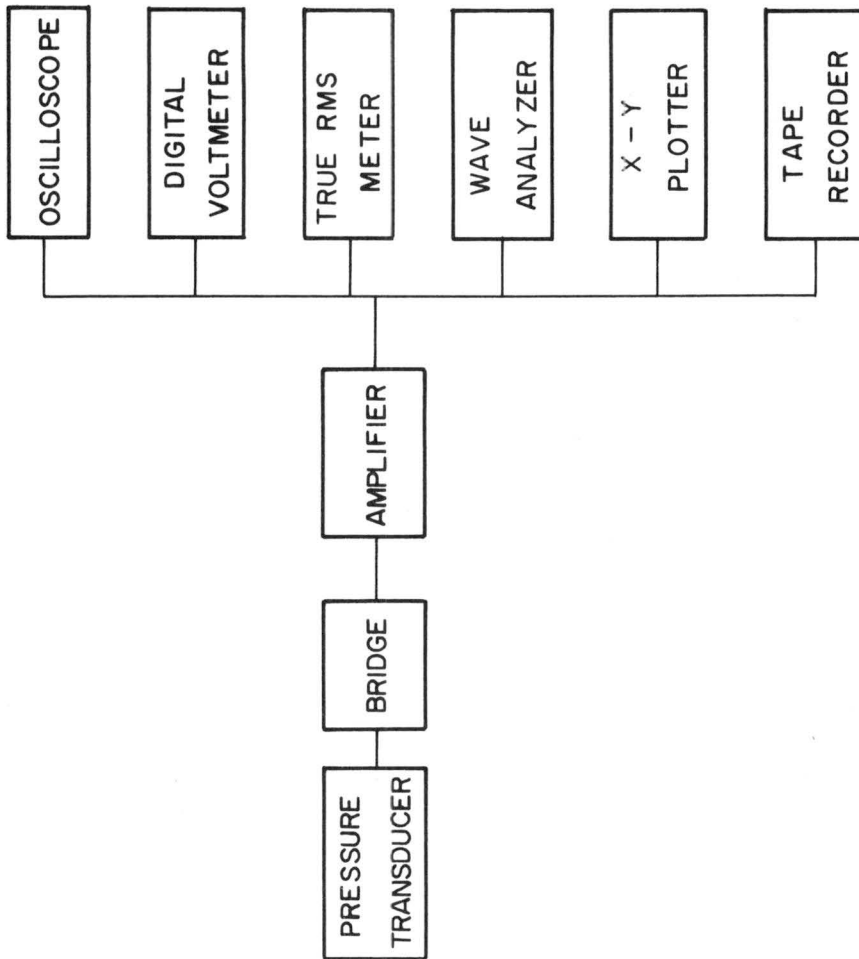


Figure 3.1 Simplified block diagram of the pressure-transducer measurement system.

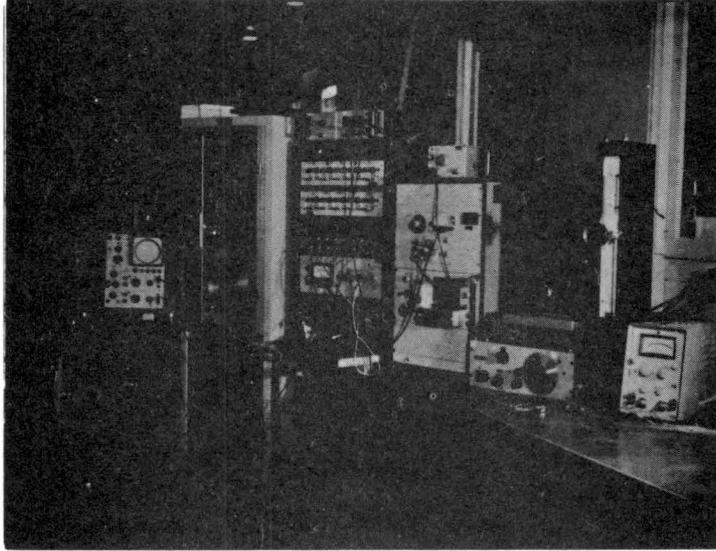


Figure 3.2 General view of the pressure measurement system.

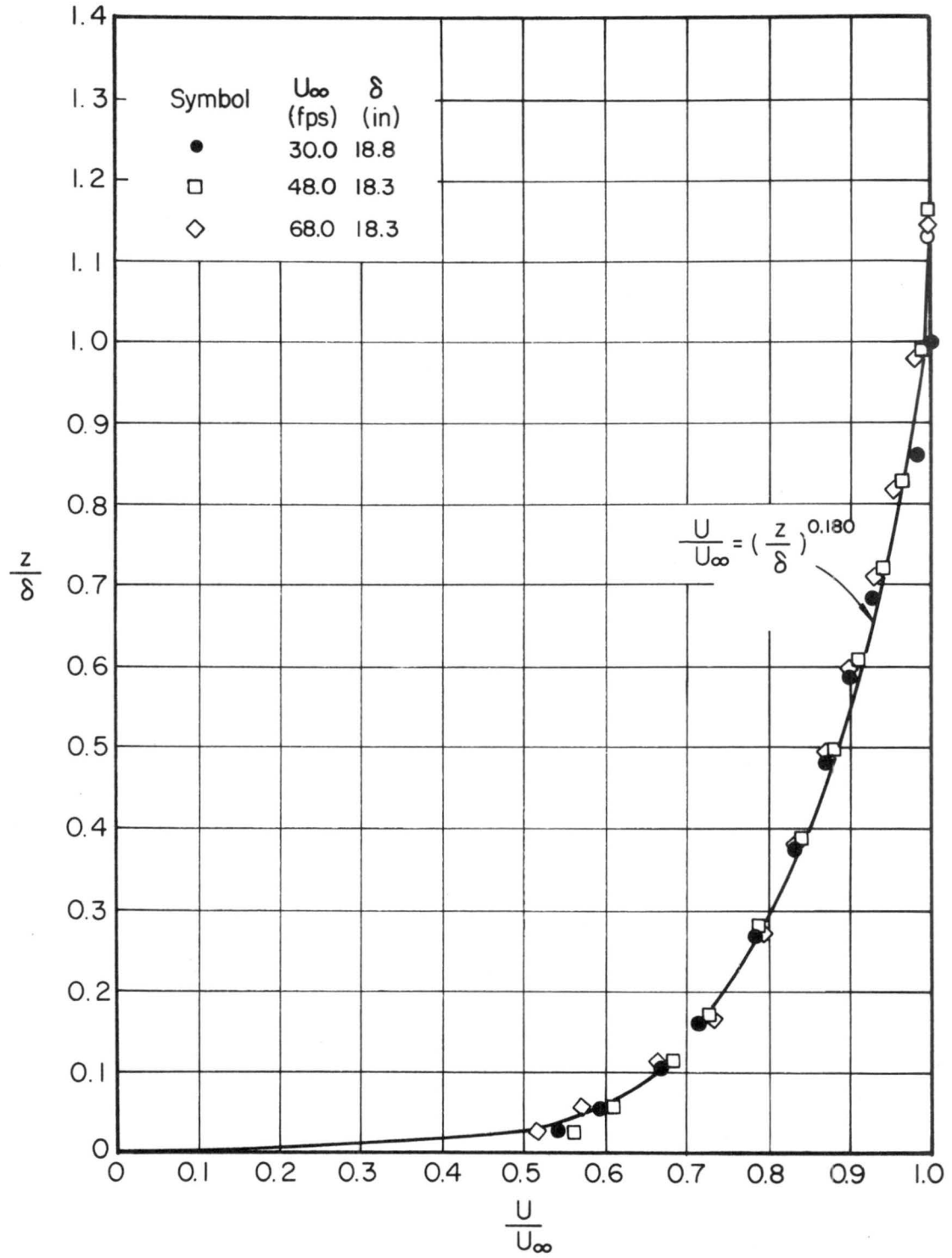


Figure 4.1 Velocity variation with height at station 1.

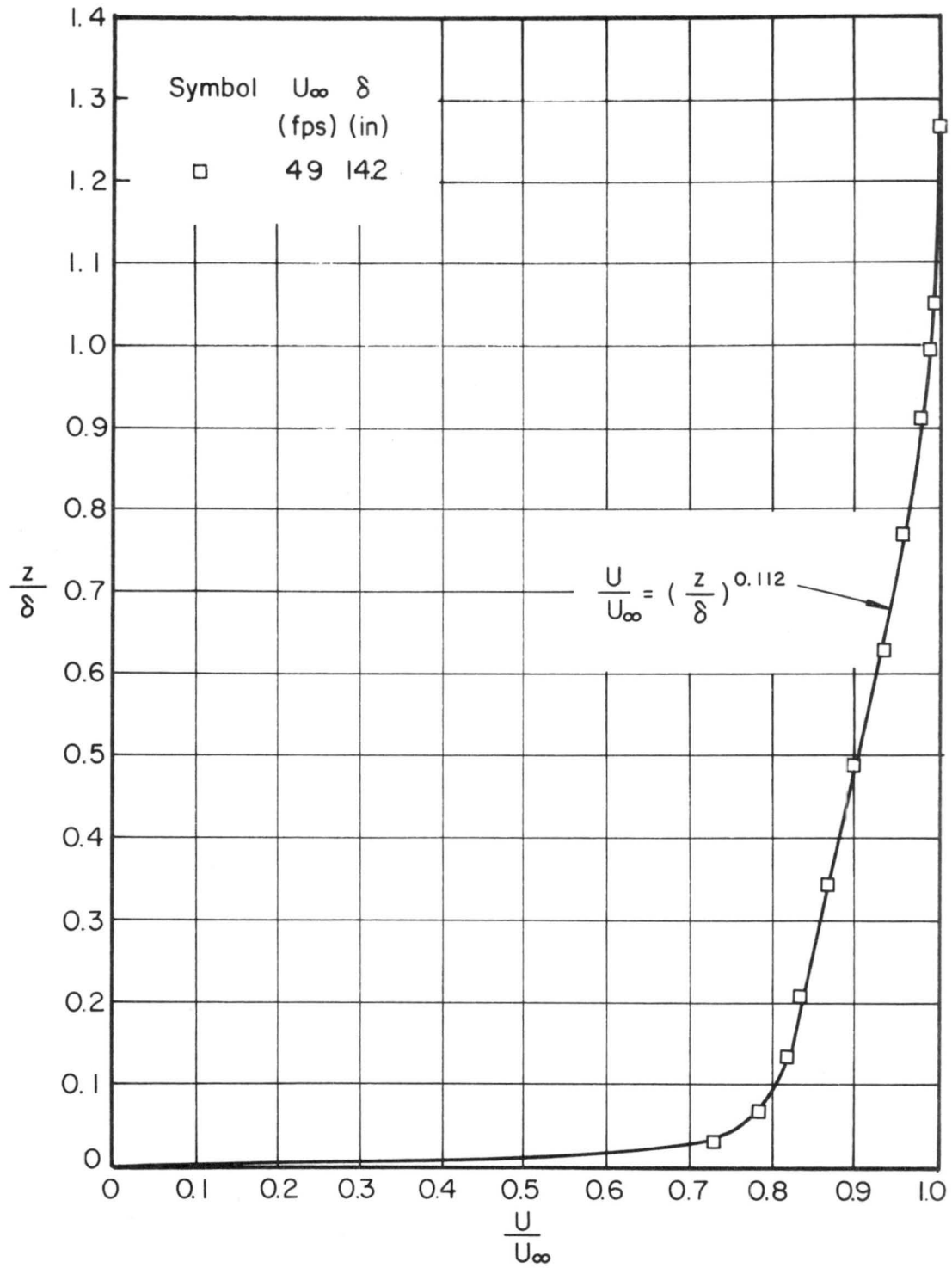


Figure 4.2 Velocity variation with height at station 2.

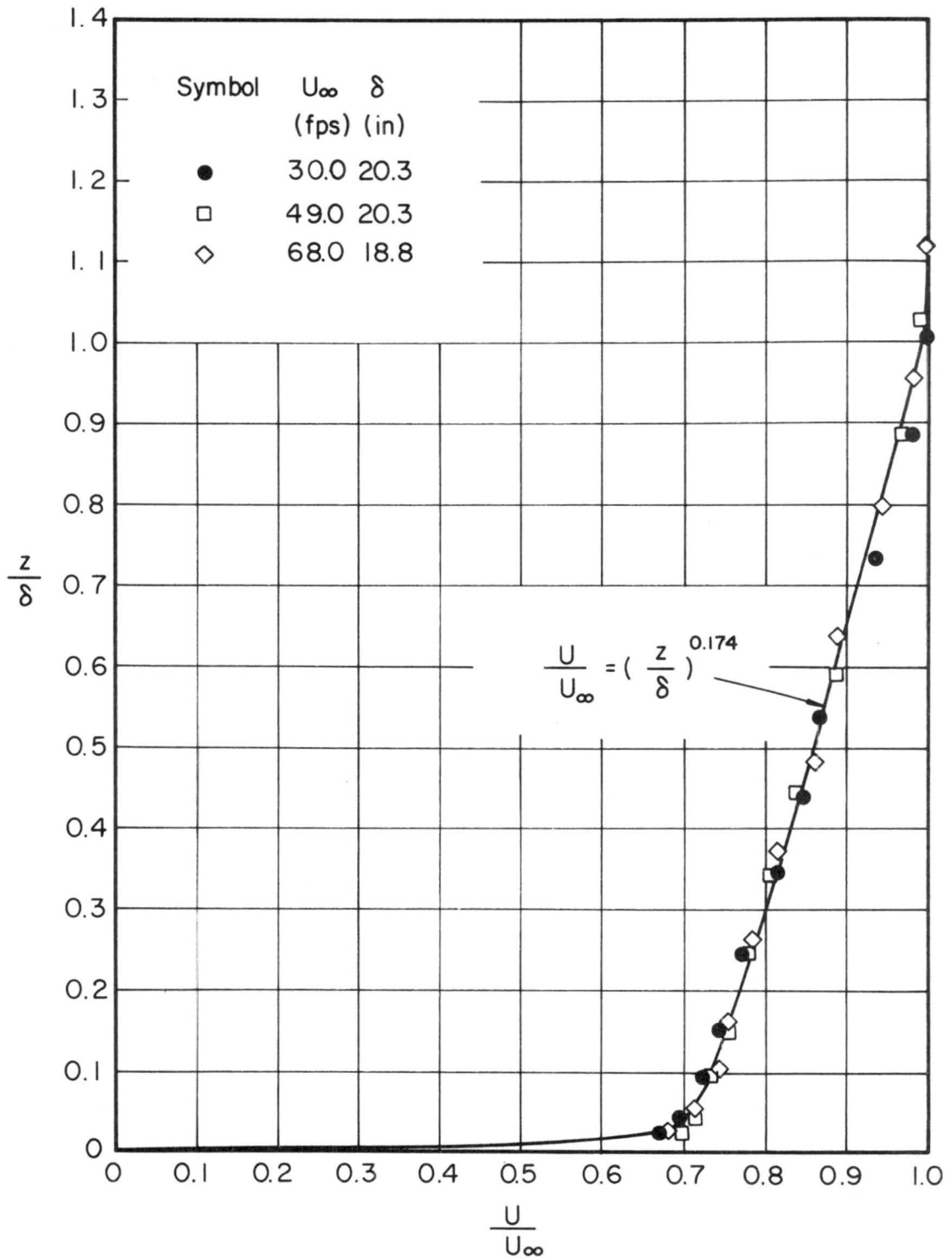


Figure 4.3 Velocity variation with height at station 3.

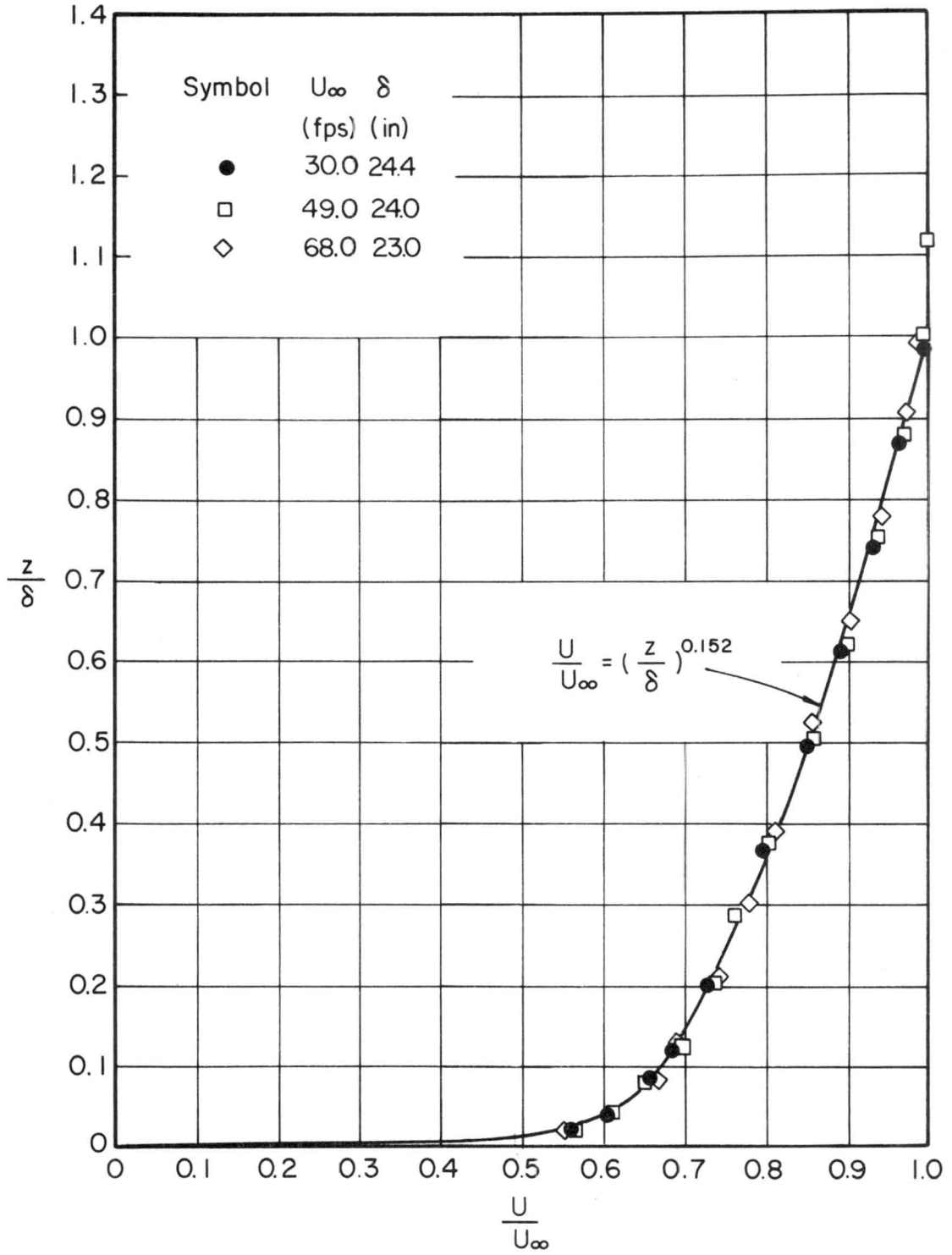


Figure 4.4 Velocity variation with height at station 4.

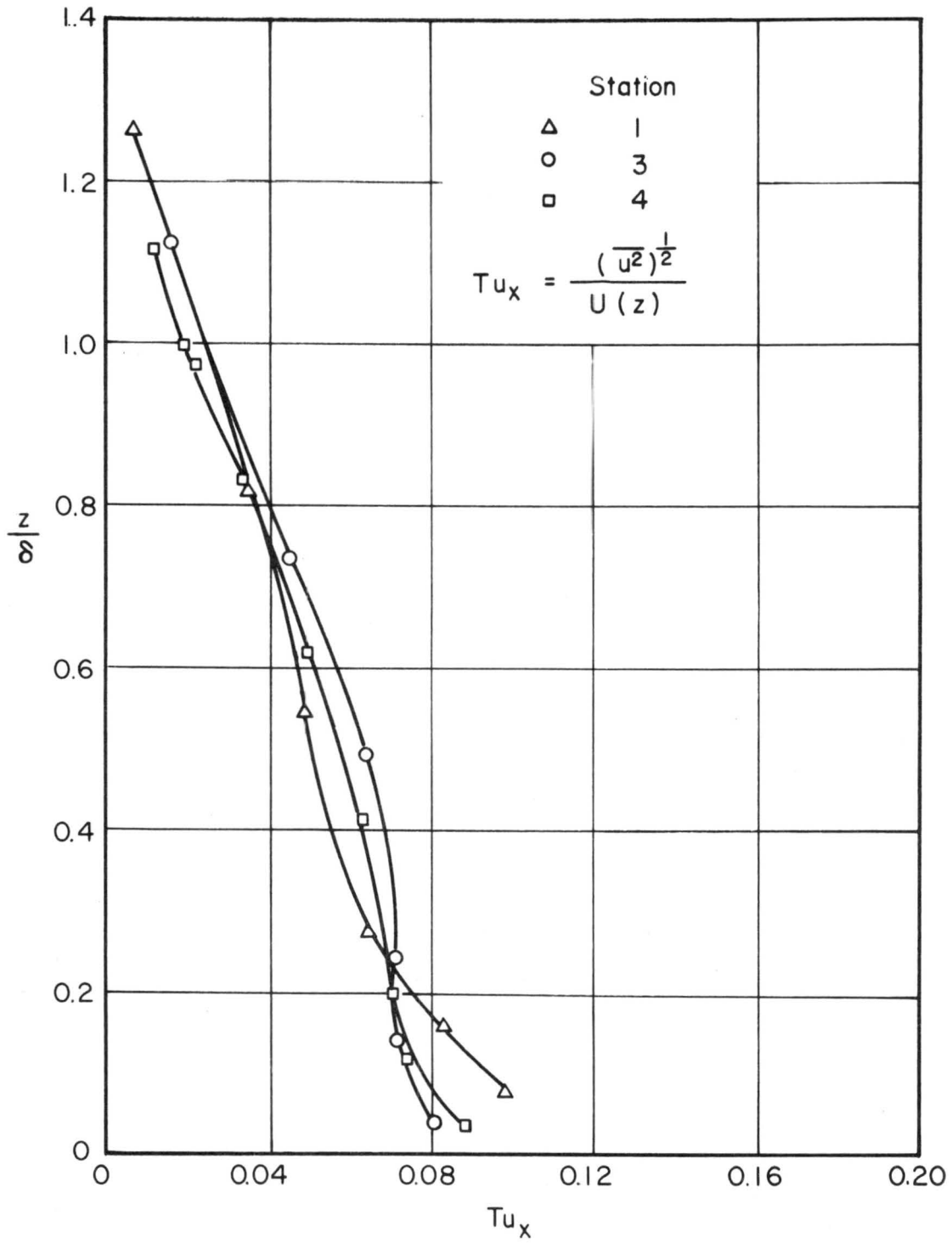
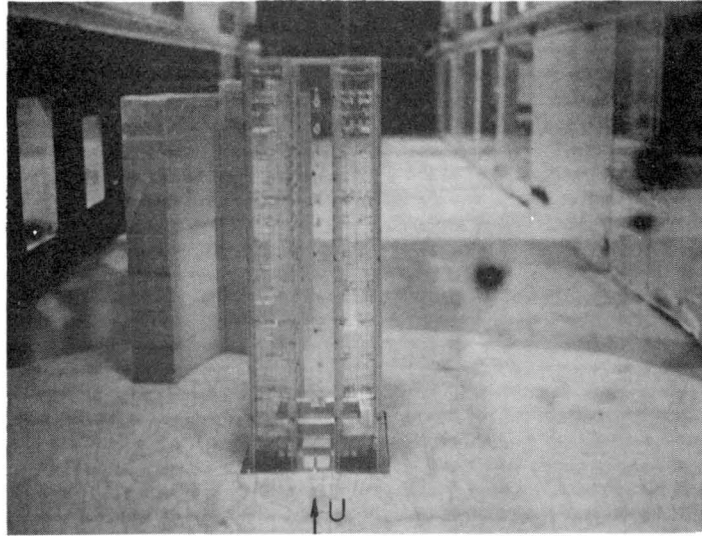
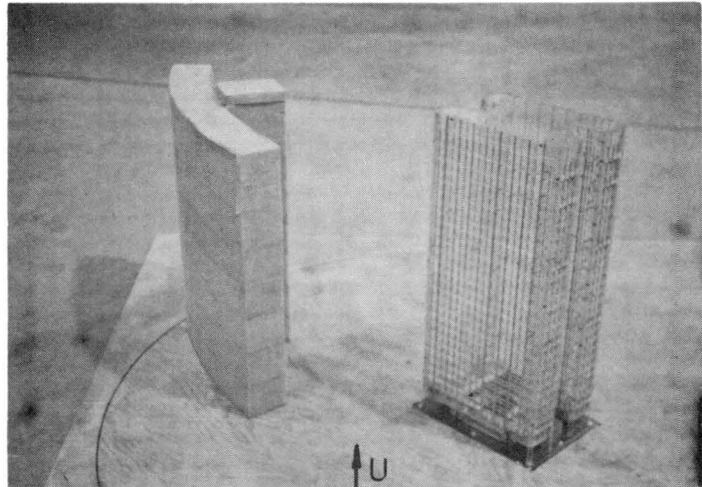


Figure 4.5 Turbulence intensity profiles along NE topography model based on local mean velocity.

N - Wind



NE - Wind



E - Wind

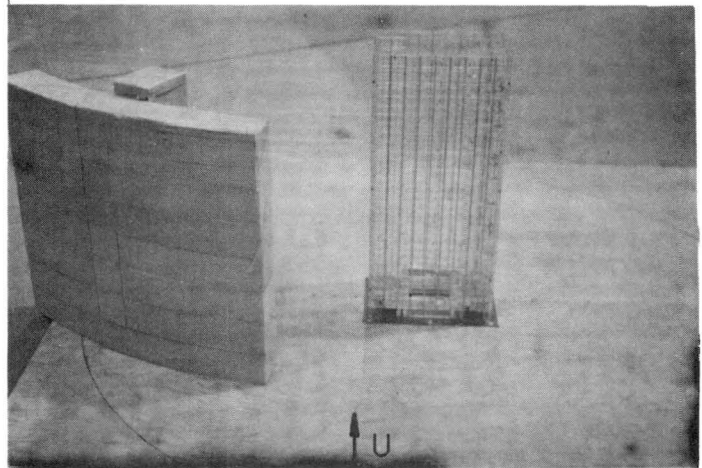
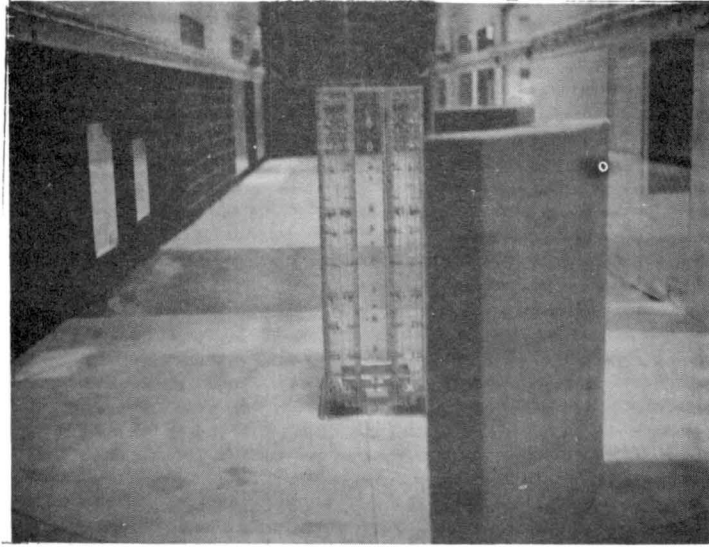
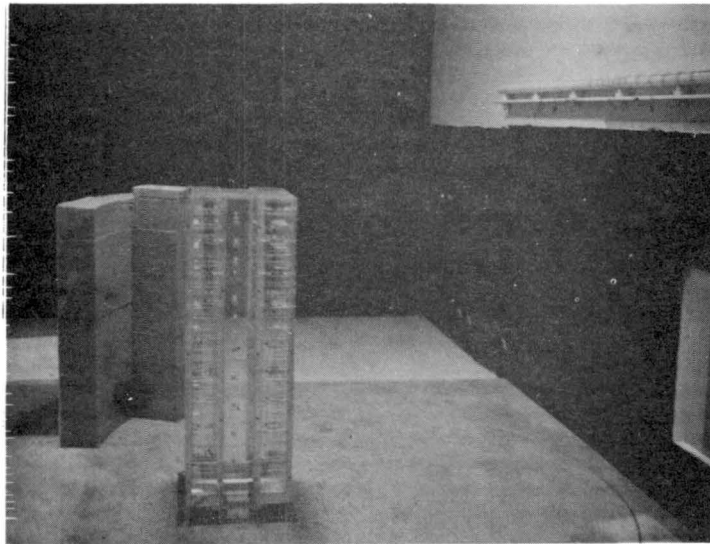


Figure 4.6 View of building model; N, NE and E wind.



View Looking Downstream



View Looking Upstream

Figure 4.7 View of building model; S wind.

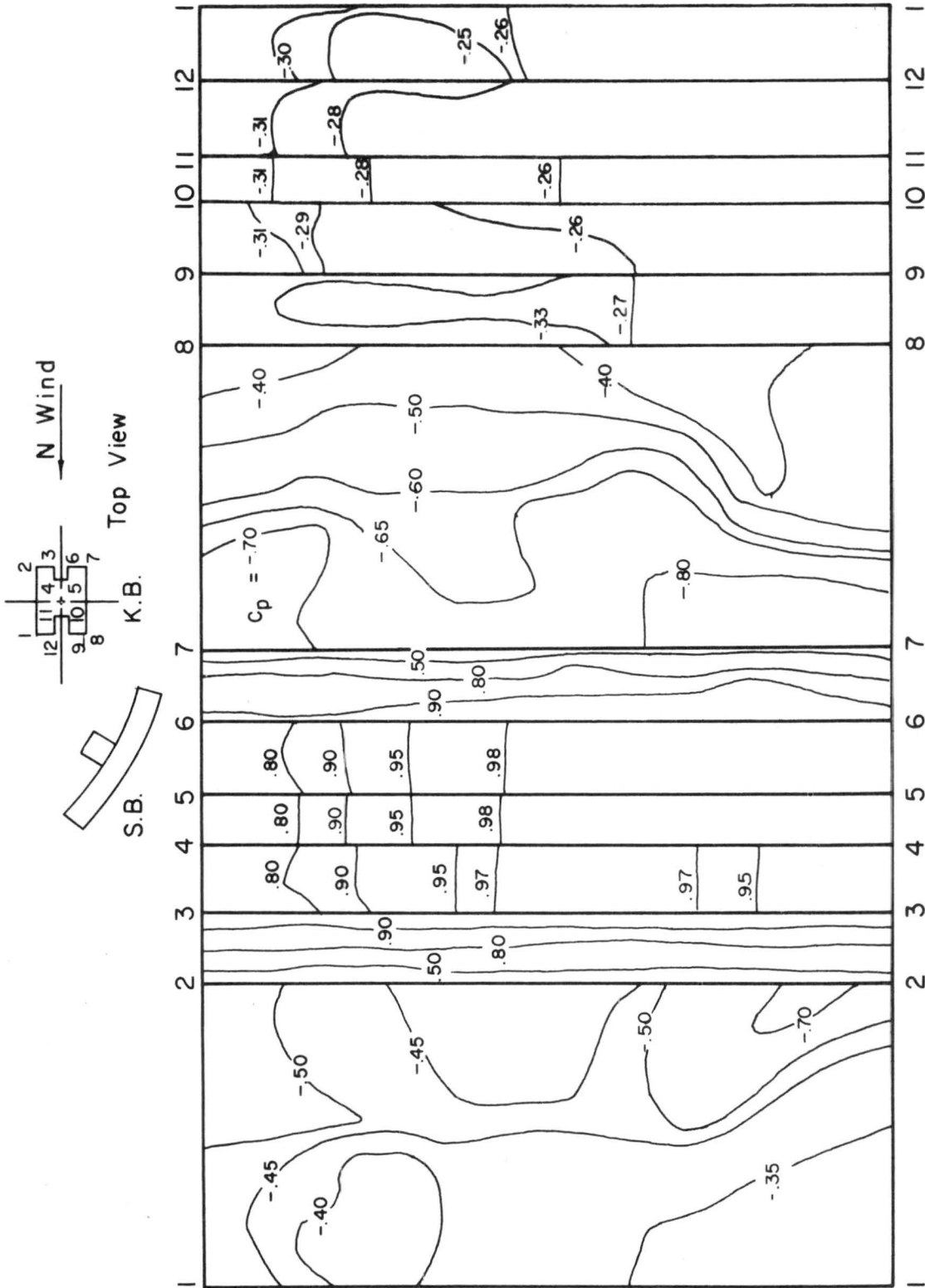


Figure 4.8 Mean pressure coefficient; N wind.

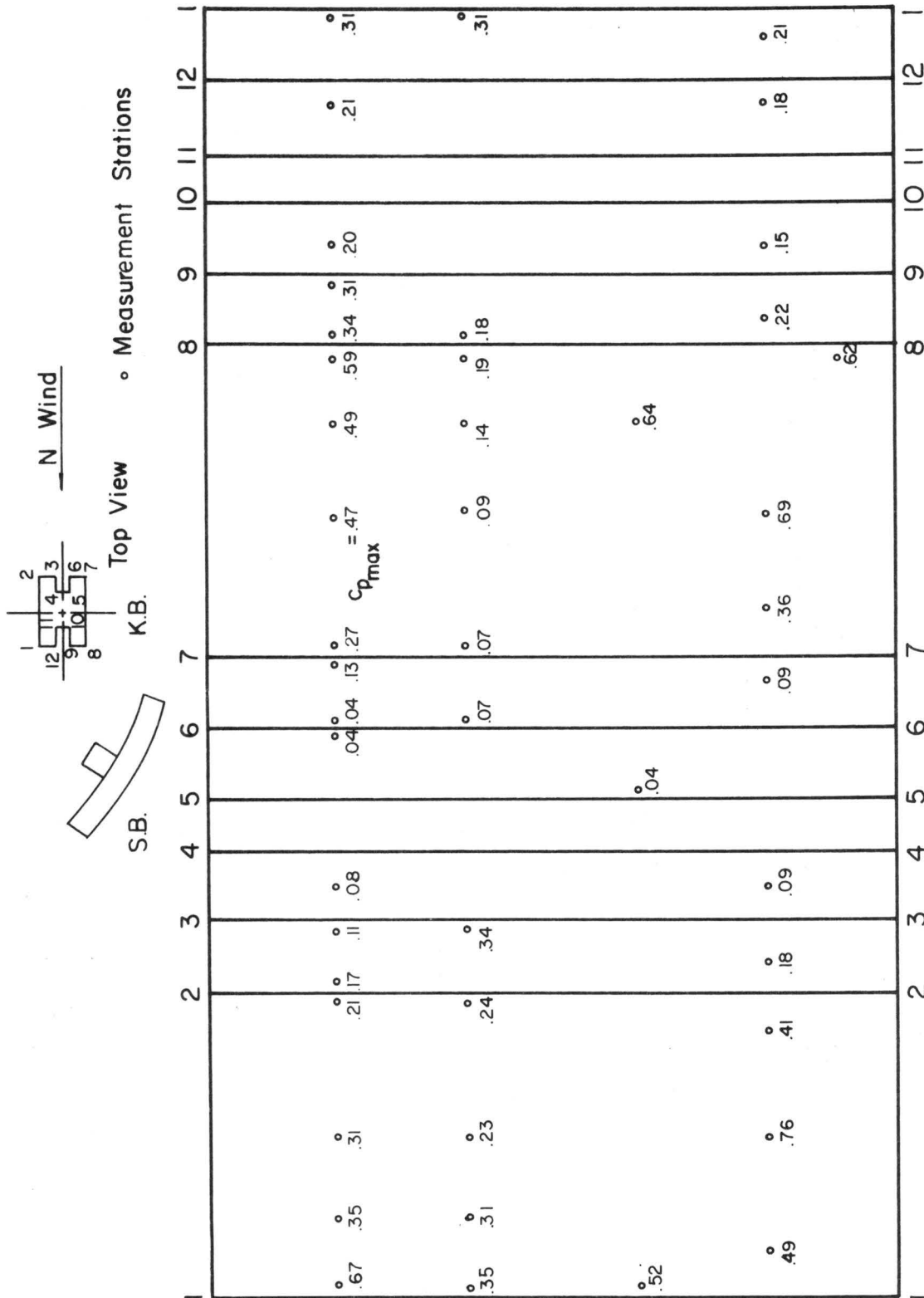


Figure 4.9 Peak pressure coefficient; N wind.

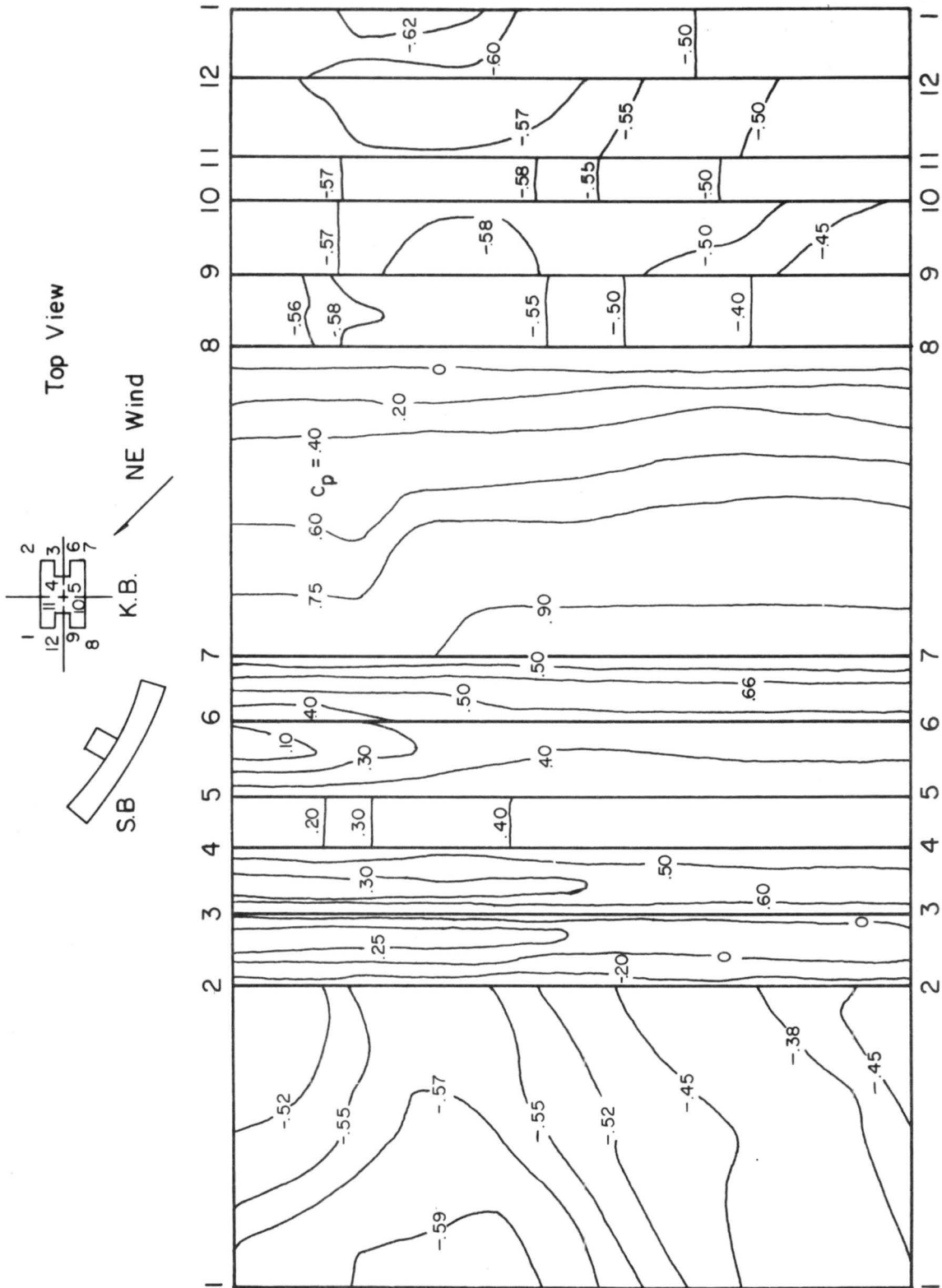


Figure 4.10 Mean pressure coefficient; NE wind.

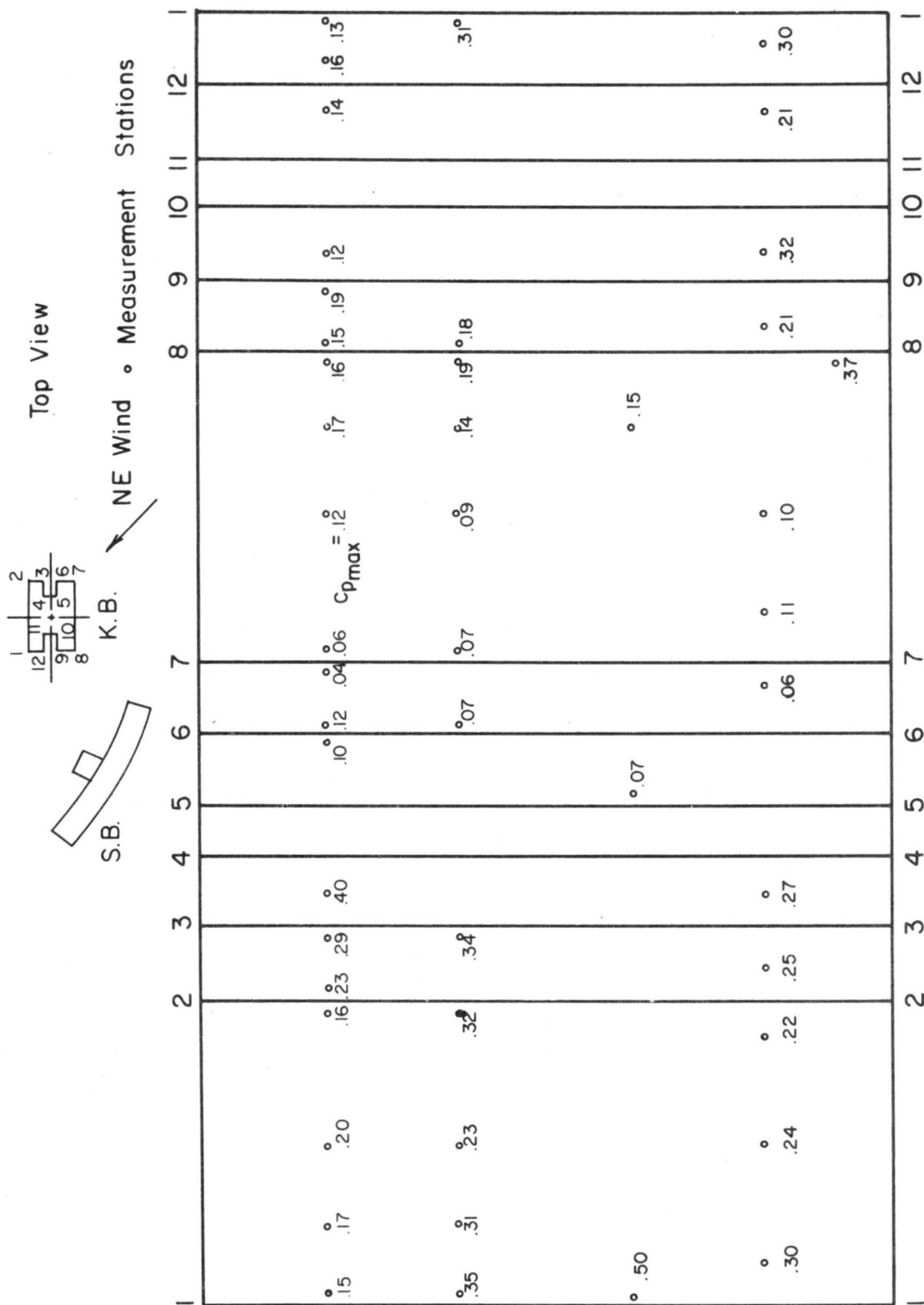


Figure 4.11 Peak pressure coefficient; NE wind.

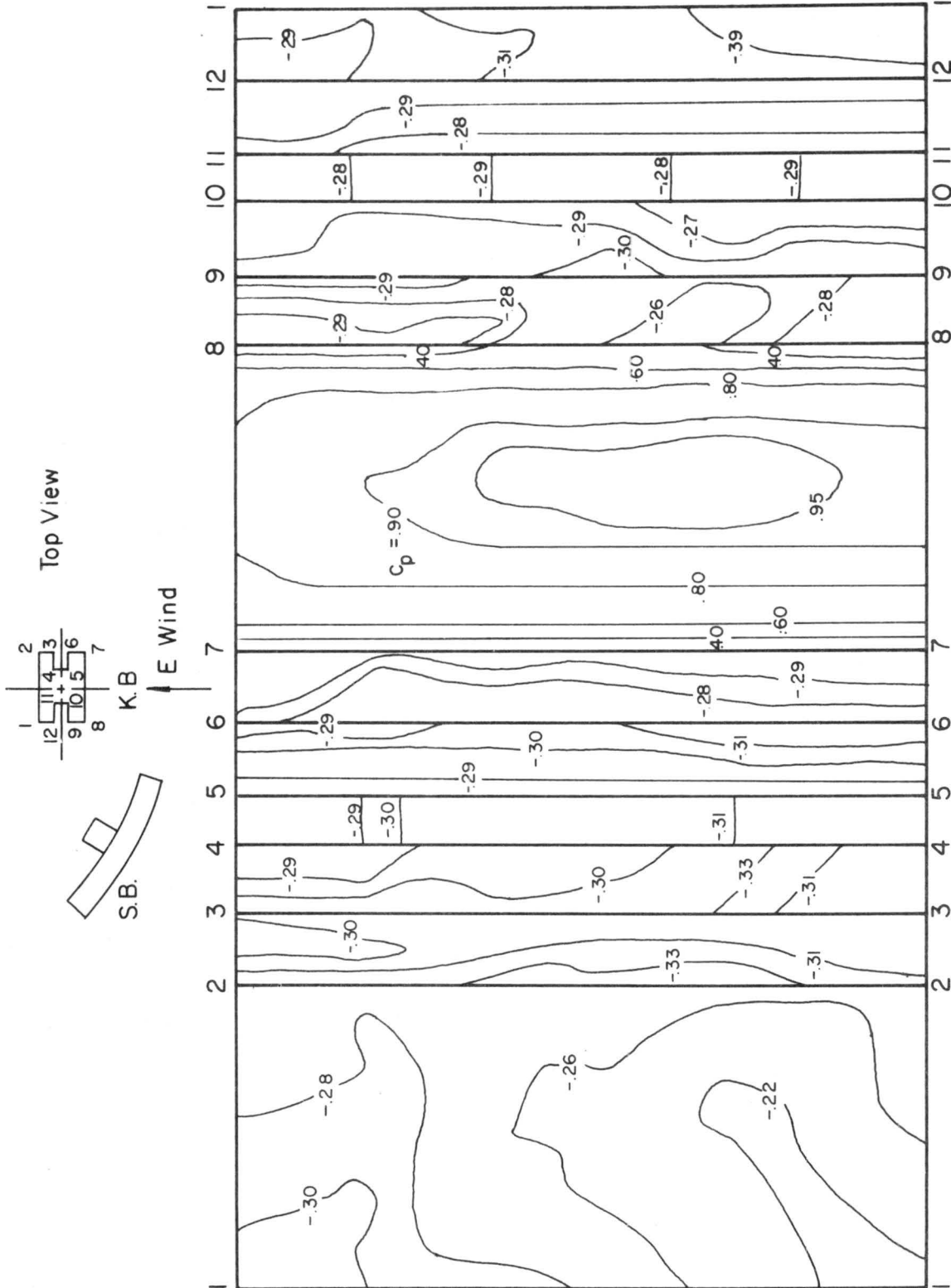


Figure 4.12 Mean pressure coefficient; E wind.

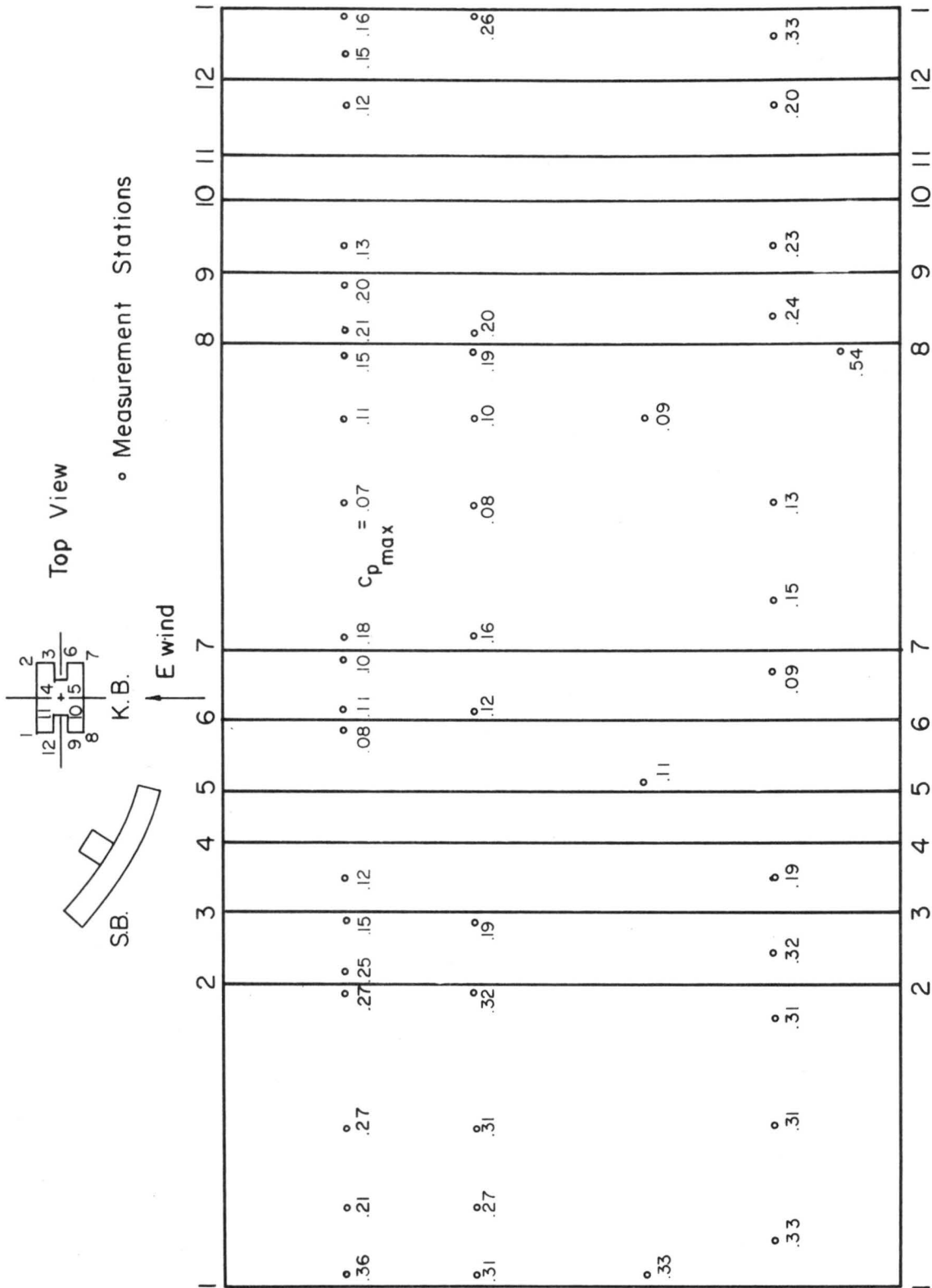


Figure 4.13 Peak pressure coefficient; E wind.

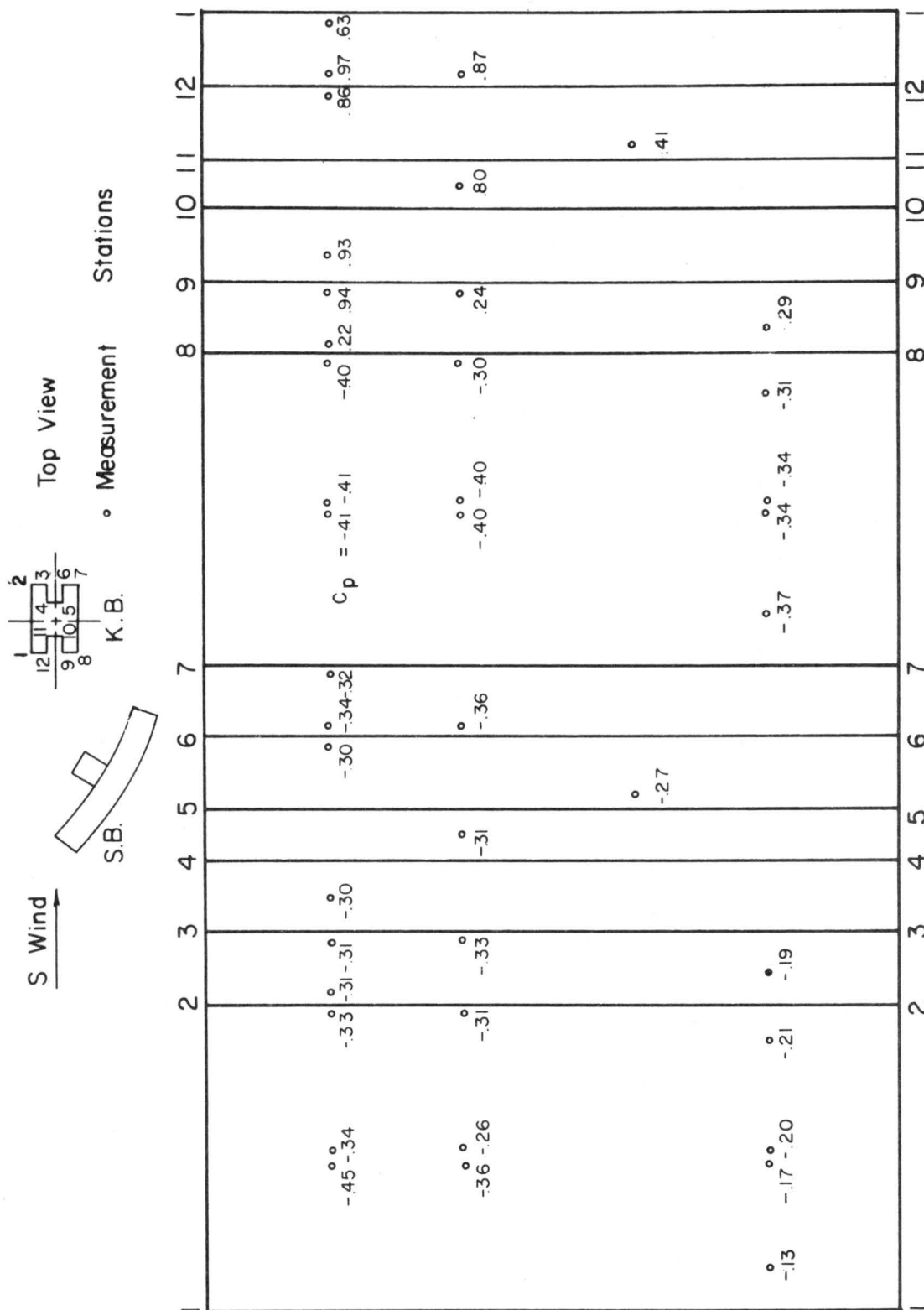


Figure 4.14 Mean pressure coefficient; S wind.

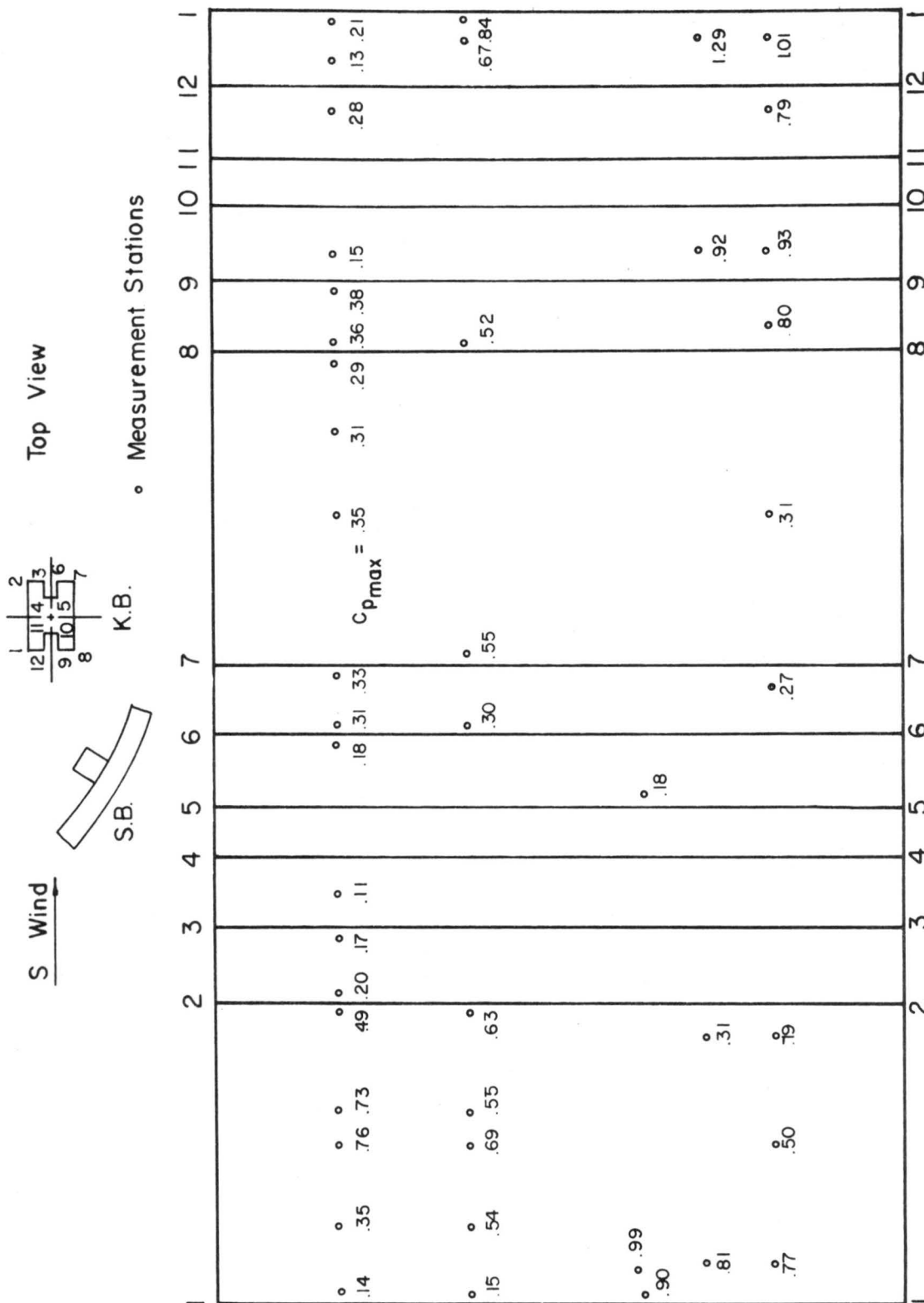


Figure 4.15 Peak pressure coefficient; S wind.

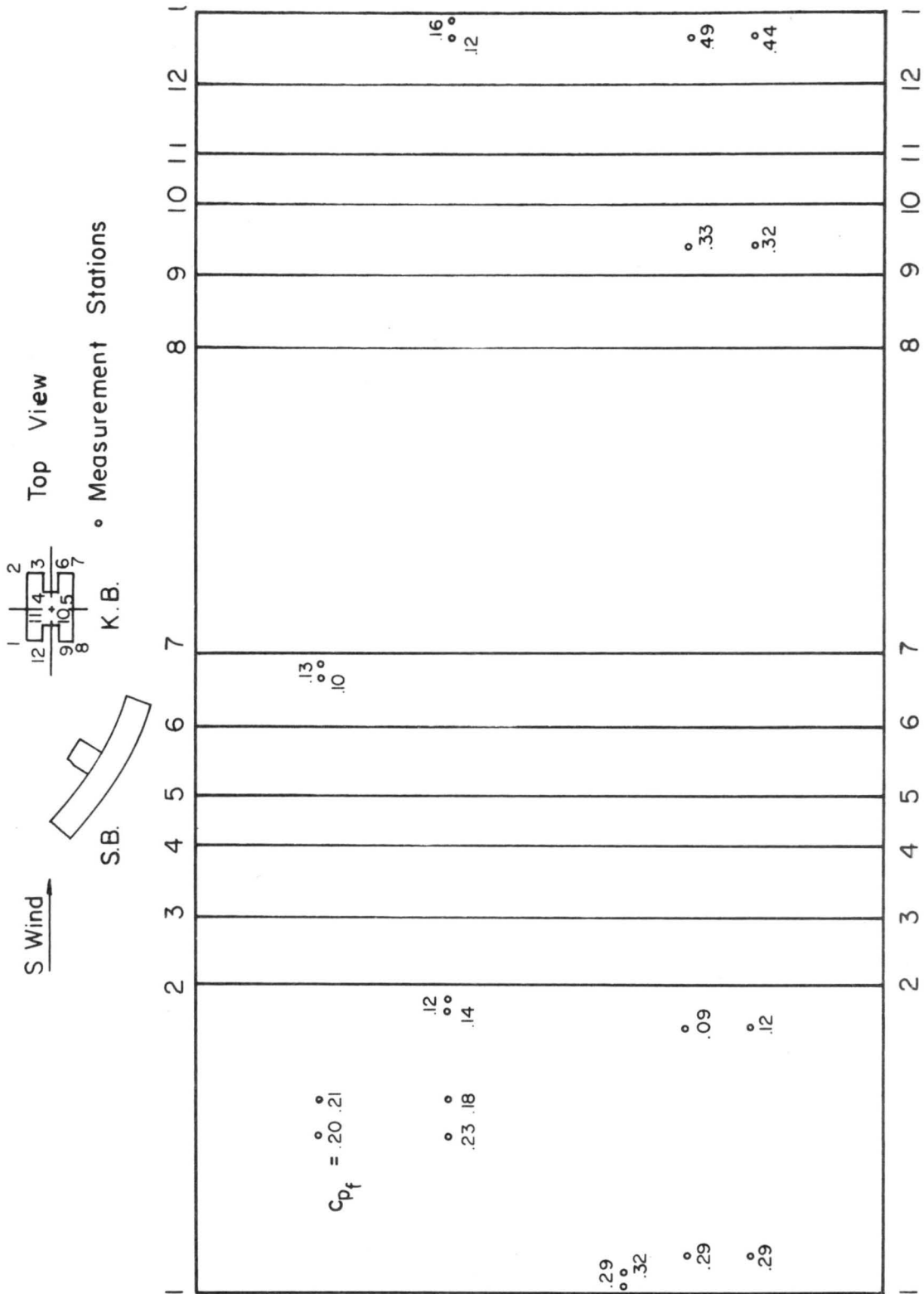


Figure 4.16 Fluctuating pressure coefficient; S wind.